Electronic Supplementary Material (ESI) for Journal of Materials Chemistry A.

Tailoring the Pt/ionomer interface for enhancing the local oxygen transport in proton exchange membrane fuel cells

Fengman Sun,[abc] Haijun Liu,[abc] Qian Di,[bc] Keyi Xu,[bc] Ming Chen,*[bc] Haijiang Wang*[bc]

[a] Harbin Institute of Technology, Harbin, 150001, China

[b] Department of Mechanical and Energy Engineering, Southern University of Science and Technology, Shenzhen, 518055, China

[c] Guangdong Provincial Key Laboratory of Energy Materials for Electric Power, Southern University of Science and Technology, Shenzhen 518055, China

Fig. S1 Hydrophobic nano-SiO_2 was obtained by modifying hydrophilic nano-SiO_2 with octamethylcyclotetrasiloxane (D4).

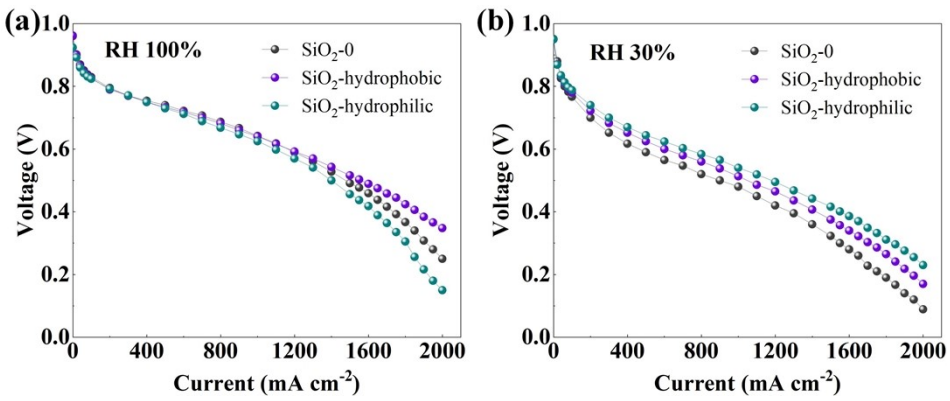

Fig. S2 Performance of MEA containing SiO_2-hydrophilic and SiO_2-hydrophobic under different relative humidity. (a) RH 100%. (b) RH 30%.

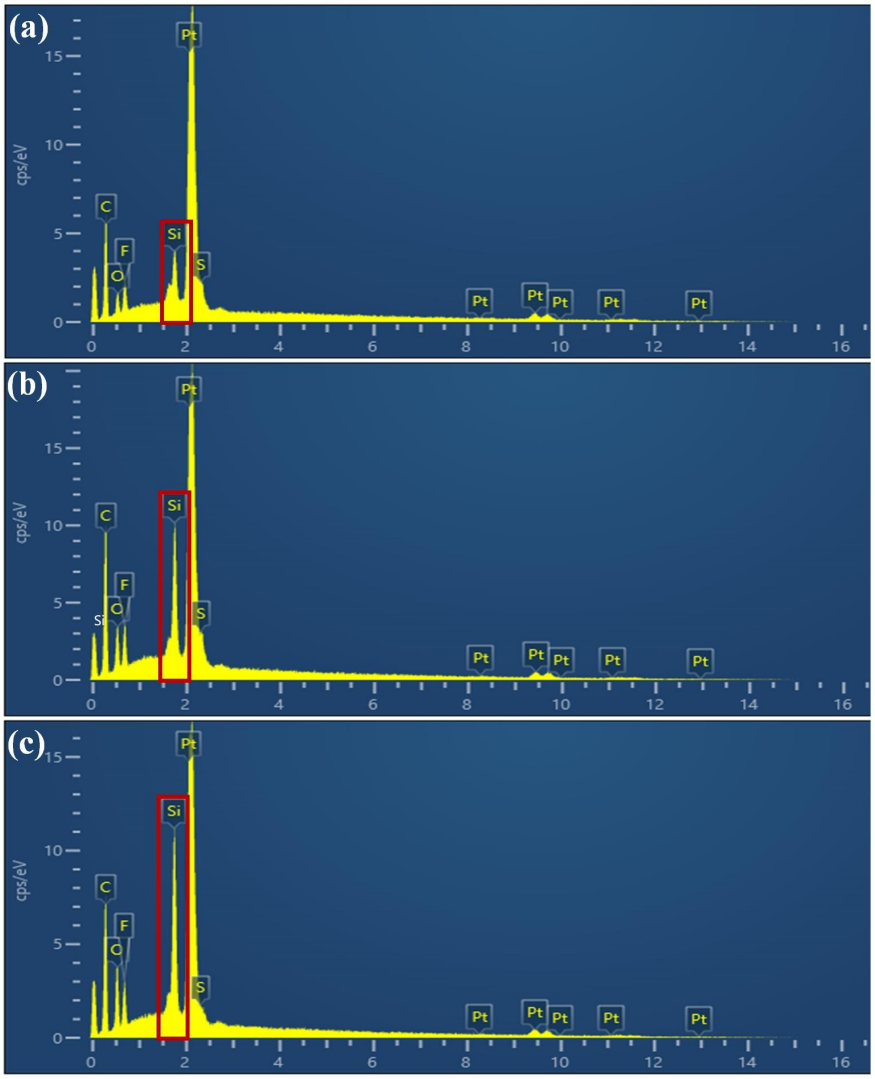

Fig. S3 The original spectra of EDS analysis for each sample, (a) SiO_2-5%, (b) SiO_2-10%, (c) SiO_2-15%.

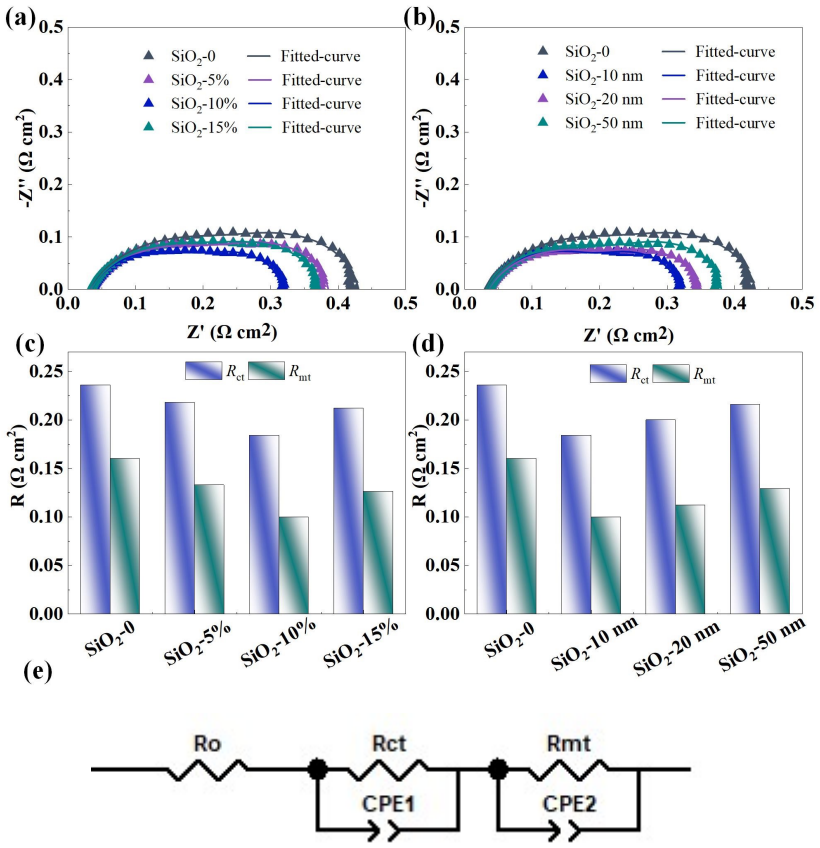

Fig. S4 EIS analysis at 1500 mA cm^{-2}. (a) and (c) The MEAs containing nano-SiO_2 with various contents. (b) and (d) The MEAs containing nano-SiO_2 with various particle sizes. (e) The equivalent circuit used to fit typical electrochemical impedance spectroscopy for PEMFCs to obtain R_{ct} and R_{mt}.

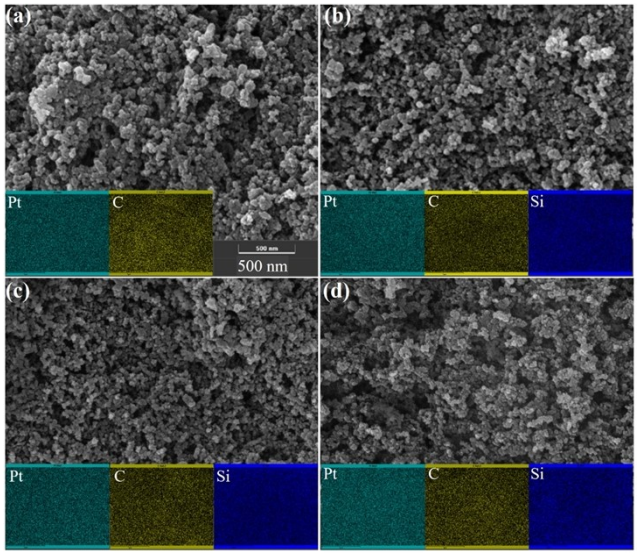

Fig. S5 SEM images of catalyst layers and the corresponding EDS mappings (insets), (a) SiO_2-0, (b) SiO_2-10 nm, (c) SiO_2-20 nm, (d) SiO_2-50 nm.

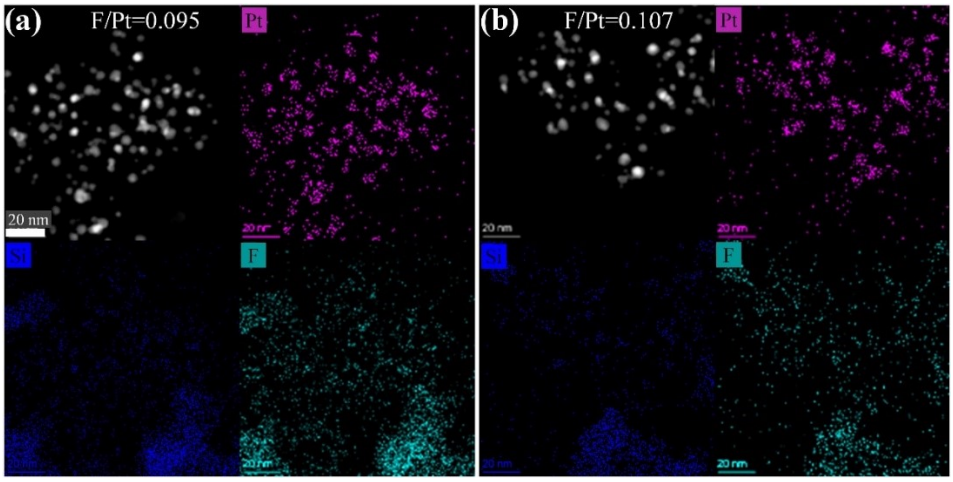

Fig. S6 STEM-HAADF-EDS analysis of catalyst layers, (a) SiO_2-20 nm, (b) SiO_2-50 nm.

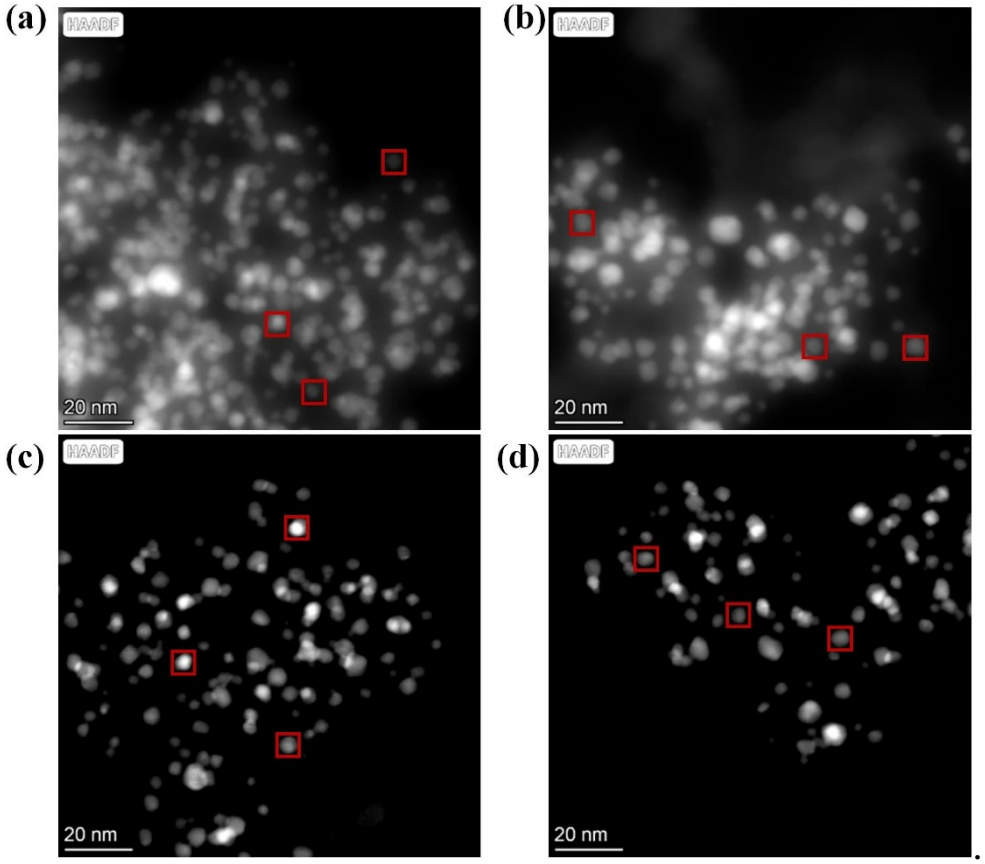

Fig. S7 The sites were marked with squares for EDS analysis for each sample, (a) SiO_2-0, (b) SiO_2-10 nm, (c) SiO_2-20 nm, (d) SiO_2-50 nm.

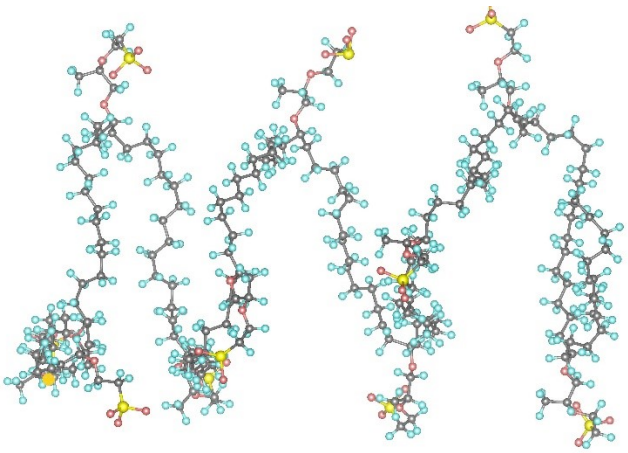

Fig. S8 Nafion ionomer, the grey, pink, yellow and cyan beads denoted C atoms, O atoms, S atoms and F atoms, respectively.

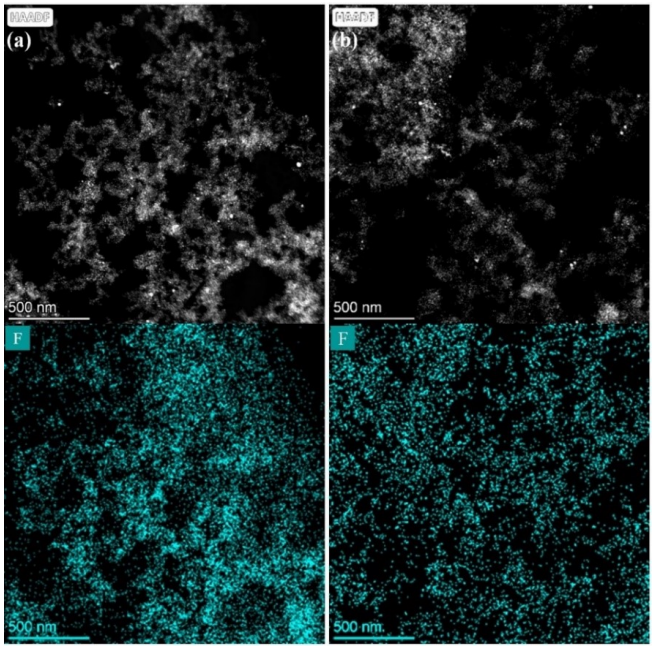

Fig. S9 STEM-HAADF-EDS analysis of catalyst layers, (a) SiO_2-0, (b) SiO_2-10 nm.

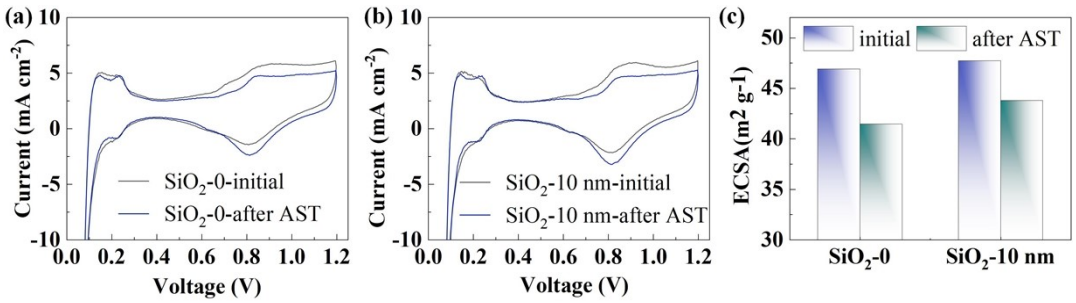

Fig. S10 The cyclic voltammetry (CV) curves were depicted before and after the AST. (a) SiO_2-0 MEA. (b) SiO_2-10 nm MEA. (c) ECSA was calculated.

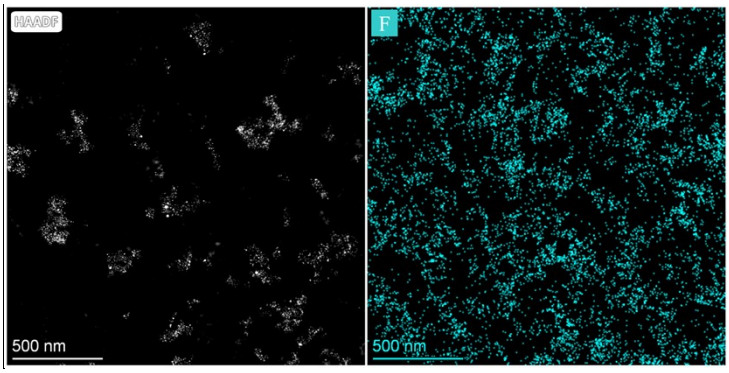

Fig. S11 STEM-HAADF-EDS analysis of SiO_2-10 nm catalyst layer after AST.

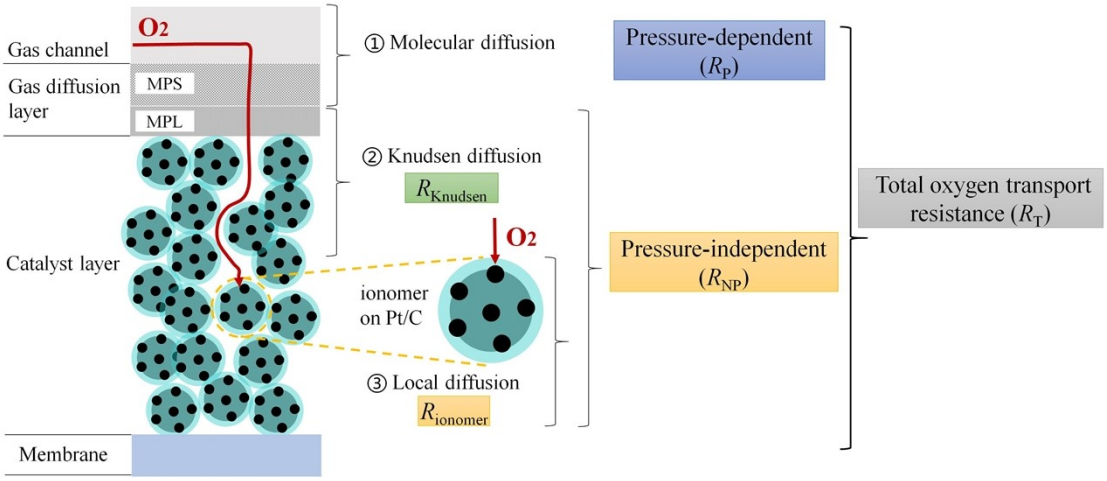

Fig. S12 Oxygen transport pathway in fuel cell.

Limiting current method was used to measure oxygen transport resistance. As shown in Fig. S11, in fuel cell cathode, oxygen passes through the gas channel in flow field plate by convection, then diffuses through gas diffusion layer (GDL) and catalyst layer (CL). In the next, oxygen dissolves into the ionomer film on catalyst surface to participate in the oxygen reduction reaction (ORR). What needs to be pointed out is gas diffusion layer (GDL) is made up of macroporous substrate (MPS) and microporous layer (MPL). The pore size of carbon paper MPS is 20-50 μm. The microporous layer is composed of carbon powder and hydrophobic agent, the pore size of which is 0.1-0.5 μm.

Total oxygen transport resistance (R_T) is converted from limiting current density. The flux of oxygen is proportional to the concentration difference of oxygen in the gas

channel ($C_{O_2,GC}$) and at the Pt reaction surface ($C_{O_2,Pt}$) . According to Faraday's law, N_{O_2} can be related to the current density.[1,2]

$$N_{O_2} = \frac{i}{4F} = \frac{1}{RT}(C_{O_2,GC} - C_{O_2,Pt}) \quad [1]$$

At limiting current density, the oxygen concentration at the Pt surface becomes zero. Consequently, R_T can be calculated from limiting current density by

$$R_T = C_{O_2,GC} \frac{4F}{I_{lim}} \quad [2]$$

$$C_{O_2,GC} = C_{inlet} = \frac{P - P_W}{RT} X_{O_2}^{dry} \quad [3]$$

$$R_T = \frac{4F}{I_{lim}} \frac{P - P_W}{RT} X_{O_2}^{dry} \quad [4]$$

R_T is the total oxygen transport resistance, T is cell temperature, P is total gas pressure, P_W is the water pressure, R is the gas constant, and $X_{O_2}^{dry}$ is O_2 molar fraction in the dry gas.

Total oxygen transport resistance (R_T) is categorized in three parts in cathode in fuel cell, referred to as R_P, $R_{Knudsen}$ and $R_{ionomer}$. Above all, R_P acts as pressure-dependent component, mainly caming from the intermolecular diffusion of oxygen passing through gas channel of polar plate and macroporous substrate of gas diffusion layer. $R_{Knudsen}$ originates from the Knudsen diffusion of oxygen in the microporous layer of gas diffusion media and catalyst layer. $R_{ionomer}$ represents the local oxygen transport resistance from Pt/ionomer interface. Knudsen diffusion coefficient and diffusion coefficient for liquid water/ionomer are independent of pressure. So, we can separate the total transport resistance (R_T) into pressure-dependent (R_P) and pressure-independent components (R_{NP}). $R_{ionomer}$ and K_{nudsen} can be distinguished from R_{NP} by temperature sensibility, since $R_{ionomer}$ is much more affected by temperature than $R_{Knudsen}$.

$$R_T = R_P + R_{NP} \quad [5]$$

$$RNP = RKnudsen + Rionomer \quad [6]$$

$$RKnudsen = AT^{-1/2} \quad [7]$$

$$Rionomer = BT^{-1}e^{17200/RT} \quad [8]$$

where R is the gas constant, A and B are the constants.

The limiting current density test was conducted under the operating conditions of low oxygen concentration, low relative humidity and large gas flow. On the one hand, the low oxygen concentration determined that the amount of water generated was small. On the other hand, the low relative humidity and large gas flow rate ensured that all the generated water was in the form of water vapor. In this case, water flooding could be avoided and the good moisture of the proton exchange membrane could be maintained, thereby ensuring the stable humidity in the fuel cell. The limiting current density test was conducted to separate various oxygen transport resistances. The test was at 75% RH with hydrogen anode and diluted oxygen cathode (2 mol % O_2 in N_2) at temperatures of 50°C, 60°C, 70°C and 80°C, and varying backpressures of 100 kPa, 150 kPa, and 200 kPa. The anode and cathode maintained constant flow rates of 1800 mL min^{-1} and 4500 mL min^{-1}, respectively. Cell current at the voltage of 0.2 V was selected as the limiting current.

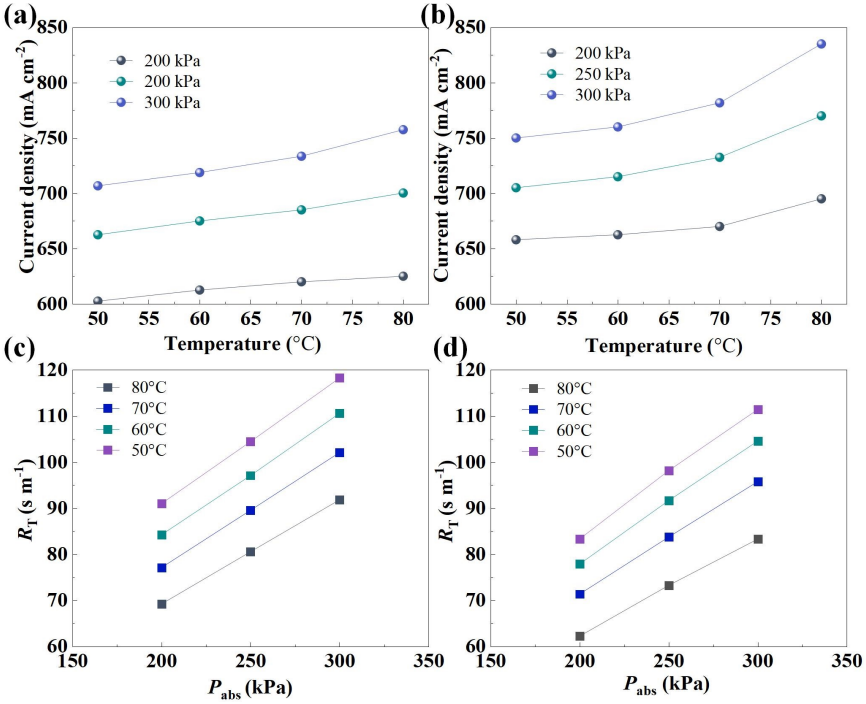

Fig. S13 The limiting current densities at different temperatures and pressures were measured. (a) and (b) were the limiting current densities of SiO_2-0 MEA and SiO_2-10 nm MEA, respectively. (c) and (d) were the R_T-P_{abs} plots of SiO_2-0 MEA and SiO_2-10 nm MEA, respectively.

After the limiting current densities at different temperatures and pressures were measured (Fig. S12a-b), R_T was calculated from the Equation [4]. A linear correlation between R_T and P_{abs} was observed in Fig. S12c-d. The R_T-P_{abs} under 60°C was selected to compare the R_T difference between SiO_2-0 and SiO_2-10 nm MEA, with R_{NP} being derived from the intercept of the R_T-P_{abs} plot, as illustrated in Fig. 3h. The difference from R_{NP} made a major contribution to the distinction of R_T in the two MEAs. According to the Equation [6]-[8], R_{NP} was fitted as $R_{Knudsen}$ and $R_{ionomer}$, as shown in Fig. 3i.

References

1 D.R. Baker, D.A. Caulk, K.C. Neyerlin, M.W. Murphy, J. Electrochem. Soc., 2009, 156, B991-B1003.

2 N. Nonoyama, S. Okazaki, A.Z. Weber, Y. Ikogi, T. Yoshida, J. Electrochem. Soc., 2011, 158, B416-B423.